Journal of Electroceramics 3:2, 163–172, 1999

Monolayer-Mediated Patterning of Integrated Electroceramics

DAVID A. PAYNE
Direct Fabrication Department, Sandia National Laboratories, Albuquerque, NM 89185-1411

PAUL G. CLEM
Department of Materials Science and Engineering and Frederick Seitz Materials Research Laboratory, University of Illinois at Urbana-Champaign, Urbana, IL 61801

Abstract. Integrated electroceramic thin-film devices on semiconducting or insulating substrate materials offer a wide variety of attractive attributes, including high capacitance density, nonvolatile memory, sensor/actuator ability, and other unique electrical, electromechanical, magnetic and optical functions. Thus the ability to pattern such electroceramic thin films is a critical technology for future device realization. Patterned oxide thin-film devices are typically formed by uniform film deposition followed by somewhat complicated post-deposition ion-beam or chemical etching in a controlled environment i.e., a subtractive method. We review here an upset technology, a different way of patterning, by an additive approach, which allows for the selective deposition of electroceramic thin layers without such post-deposition etching. In this method, substrate surfaces are selectively functionalized with hydrophobic self-assembled monolayers to modify the adhesion of subsequently deposited solution-derived electroceramics. The selective functionalization is achieved through microcontact printing (μ-CP) of self-assembled monolayers of the chemical octadecyltrichlorosilane on substrates of current technical interest. Subsequent sol-gel deposition of ceramic oxides on these functionalized substrates, followed by lift-off from the monolayer, yields high quality, patterned oxide thin layers only on the unfunctionalized regions. A variety of micron-scale dielectric oxide devices have been fabricated by this method, with lateral resolution as fine as 0.5 μm. In this paper, we review the monolayer patterning and electrical behavior of several patterned electroceramic thin films, including $Pb(Zr,Ti)O_3$ [PZT], $LiNbO_3$, and Ta_2O_5. A multilevel example is also given which combines selective MOCVD deposition of metal electrodes and sol-gel patterned PZT for Pt//PZT//Pt//Si(100) ferroelectric memory cells.

Keywords: chemical solution processing, self-assembled monolayers, microcontact printing, PZT, $LiNbO_3$, Ta_2O_5.

1. Introduction

The ability to pattern oxide thin films into complex structures is an area of active research, required for specific applications in electronics including use as capacitors, actuators, sensors, electrochromics, memory cells and MEMS devices [1]. For these applications, the ability to rapidly pattern electroceramic films into fine scale device architectures without deleterious effects on properties is a key concern. For many materials, the process of blanket material deposition, photolithographic resist patterning, and subtractive etching is an effective patterning method. However, the inherent chemical stability and refractory nature of many ceramics often presents difficulty for this conventional process. Subtractive patterning methods often use reactive ion etching (RIE) and wet chemical etching, which

Supported by U.S. Department of Energy, Division of Materials Sciences, under Grant No. ER 9645439, and NEDO.
Sandia is a multiprogram laboratory operated by Sandia Corporation, a Lockheed Martin Company, for the U.S. Department of Energy under contract DE-AC04-94A185000.

increase the complexity of processing since they may require controlled environments, they may etch anisotropically, and leave residual chemical artifacts related to SF_6, HF, HCl, or other etchant species [2]. The capability of avoiding such methods is especially attractive for such materials as $LiNbO_3$, which are difficult to etch (Å/s etch rates [3]) by the above methods, and for PZT, which often requires dedicated RIE equipment to avoid deleterious lead contamination. Recent work with self-assembled monolayers suggests promise for patterning the *initial* deposition of inorganic phases by surface functionalization of substrates, thereby avoiding etching requirements. The application of such monolayers to the patterning of solution-derived electroceramic thin layers is now discussed.

2. Self-Assembled Monolayers and Patterning Methodologies

The capability of moderating the adhesion/adsorption of materials on surfaces can be dependent on the robust, hydrophilic or hydrophobic nature of self-assembled monolayers, and their ability to alter substrate surface properties. Self-assembled monolayers (SAMs) of octadecyltrichlorosilane (OTS) were first reported by Sagiv [4] in 1980, and these monolayers have since found diverse applications in surface passivation (corrosion resistance), friction modification (tribology), biosensing, and nanoscale control of chemical reactions [5]. The unusual feature of such monolayers lies in the ability to order into dense, continuous, and somewhat chemically and thermally robust layers, thus allowing global changes in surface character due only to formation of a typically 10–30Å self-assembled monolayer. Two common types of monolayers, alkanethiols and organosilanes, and the manner in which such monolayers self-assemble, are illustrated in Fig. 1. The monolayers can be generally characterized as consisting of an anchor sulfur (alkanethiol SAMs) or silicon (organosilane SAMs) ion, an organic $[-(CH_2)_n-]$ chain of 6–30Å in length, and an end-functional group that may be either hydrophilic or hydrophobic. One major advance in monolayer preparation is the ability to deposit SAMs from dilute solutions in simple solvents such as hexane, ethanol, or acetone, as originally reported by Nuzzo and Allara [6] for thiol SAMs. Spontaneous organization of these films was observed to occur while in solution, resulting in monolayer film heights of 4–21Å for theoretical molecular lengths of 6–25Å, which indicates the molecules stand near-normal to the substrate surface, fully extended. Infrared data indicated the monolayers are at full extension due to molecular packing, similar to the zigzag bonding and arrangement indicated in the cartoon of Fig. 1. The key finding is that self-assembled monolayers are ordered, close-packed molecular assemblies, even if not perfect compared to single crystals.

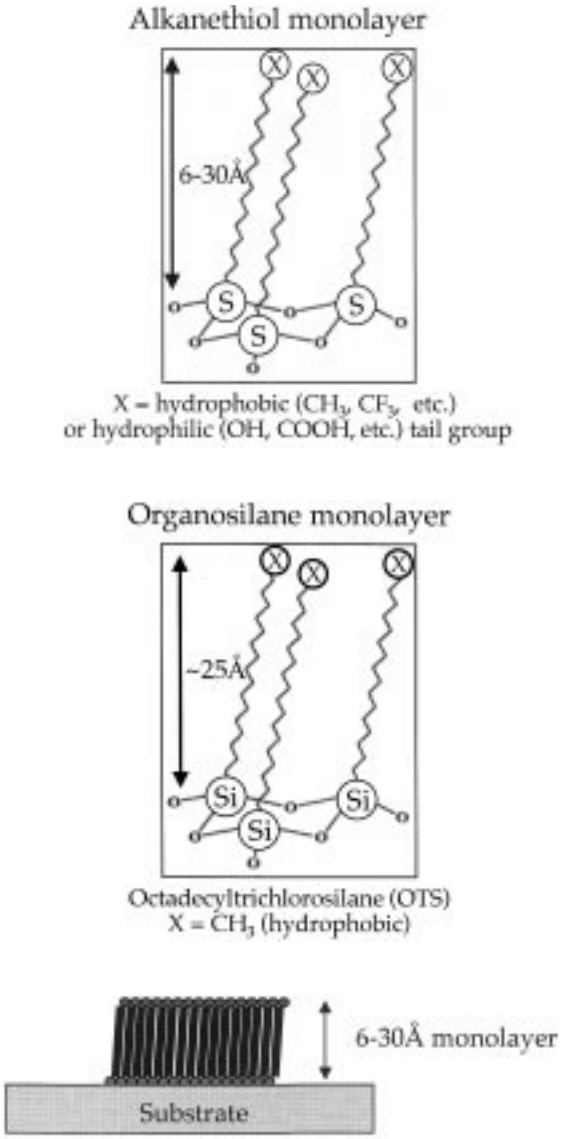

Fig. 1. Illustration of thiol and organosilane monolayers, and self assembly on a substrate.

The end group of such monolayers, denoted as X in Fig. 1, may be tailored to be either hydrophobic (e.g., $-CH_3$) or hydrophilic (e.g., $-OH$, $-COOH$), thus enabling control of surface reactivity by monolayer functionalization. Major advances have been reported by Whitesides and co-workers [7–14], Bunker et al. [15], and Collins et al. [16] on the ability to pattern such monolayers at the submicron scale, achieving selective functionalization. While other methods form complete monolayers and can later selectively remove regions by either ultraviolet exposure [16], or charged beams [8,15], the method of microcontact printing developed by Whitesides and co-workers [7,9–14] selectively deposits monolayers by a method akin to contact printing onto paper, or stamping, but on submicron to multicentimeter size scales. The method of μ-CP consists of five steps: (i) ultraviolet/electron beam lithography and removal of $\sim 1\,\mu$m thick photoresist atop a substrate, (ii) curing of a cross-linkable polymer atop this patterned photoresist, (iii) removal of the elastomeric polymer stamp from this surface, (iv) coating of the stamp with a dilute (~ 10 mM) monolayer solution in a solvent, and (v) stamping of this solution to deposit self-assembled monolayers on substrate surfaces (Fig. 2).

In our research, printed organosilane monolayers were used to modify the surface wetting and tribological interaction of substrates with solution-deposited ceramic thin film precursors. Whereas, thiol monolayers self-assemble readily above gold substrates, organosilanes (e.g., octadecyltrichlorosilane, an 18-chain organosilane) order on a wide variety of substrate materials. This opens up new opportunities for the integration of a wide variety of electroceramic devices by OTS and related methodologies.

3. Electroceramic Materials Patterning

The protocol developed for monolayer-mediated selective deposition of solution-derived oxide thin films is illustrated in Figs. 2 and 3. Stamps for this process were created by curing of polydimethylsiloxane (PDMS) over etched photoresist according to the method of Kumar and Whitesides [7], producing stamps with $\sim 1\,\mu$m raised features of potentially 40 nm to 4 cm in possible lateral dimension [12]. A 10 mM solution of octadecyltrichlorosilane (OTS) in hexane was applied to the PDMS stamp by using a photoresist spinner (3000 rpm for 30 s) and dried in a stream of research-purity Ar. Substrates were cleaned by deionized water, acetone, and isopropanol, and dried under a stream of Ar. The stamp was brought into contact with the substrate by hand for ~ 30 sec, forming microcontact printed, self-assembled monolayer patterns.

Sol-gel precursors for PZT [17,18], $LiNbO_3$ [19–21], and Ta_2O_5 [22] were spin coated atop such monolayer patterned substrates, which included Si, Al//Si, Pt//Ti//Si, sapphire, glass, and other materials. In a typical deposition, a patterned substrate was flooded with 200 μl of 0.3 M solution precursor and

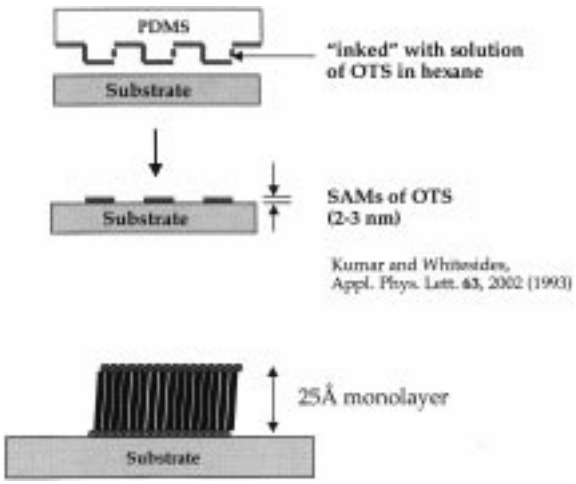

Fig. 2. Schematic outline of monolayer microcontact printing (μCP)[7].

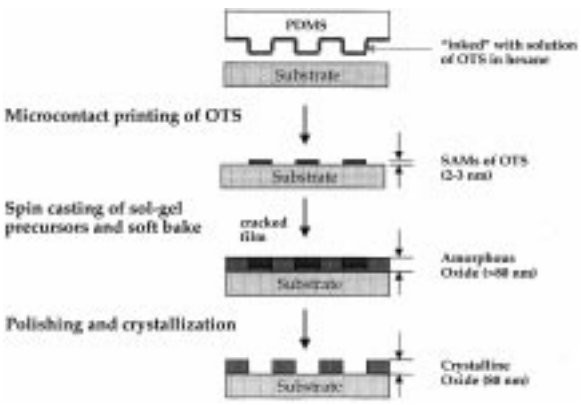

Fig. 3. Schematic of μCP monolayer patterning of sol-gel oxide thin films.

spin coated at 3000 rpm. After pyrolysis of organics by placing the substrate on a preheated 200°–300°C hot plate, films of 80–100 nm thickness were obtained. To effect lift-off of the oxide formed above monolayer-functionalized regions, these films were then washed with isopropanol or gently polished with a nonabrasive cloth (i.e., Metcloth, Buehler Corp.), wet with isopropanol. Following lift-off, during which the film deposited atop monolayer-functionalized regions de-adhered, the patterned films were further densified and crystallized by rapid heating to 700°C. Patterning of electrooptic ($LiNbO_3$), dielectric (Ta_2O_5), and switchable ferroelectric materials was readily achieved by following this protocol [18,21–22].

Monolayer-Mediated Selective Deposition of $LiNbO_3$

As described above, microcontact printing allows for the submicron scale patterning of surfaces with monolayers, thereby altering the chemical nature of such functionalized surfaces [7,9,14]. Octadecyltrichlorosilane was chosen as a hydrophobic monolayer, to provide contrast with the comparatively hydrophilic surfaces of oxide and metal substrates. Functionalized substrates bore $\sim$ 25Å monolayers of this siloxane after stamping, as determined by optical ellipsometry and atomic-force microscopy (AFM). Figure 4 illustrates a 25Å stripe of OTS as revealed in the topography mode of AFM. Monolayers used in this study were found to maintain their hydrophobic functionalization to 400°C, as determined by observation of the surface wetting angle of water droplets prior to and after annealing of monolayer-functionalized surfaces.

The method used to deposit thin layers atop these monolayers was consistent for all solutions, and involved several steps: preparation of a dilute alkoxide precursor solution, spin coating onto OTS microcontact printed substrates, low-temperature heat treatment, removal of delaminated oxide, and a final high-temperature heat treatment. The results of this processing for $LiNbO_3$ on SiO_2/Si are shown in Figs. 5a–d. Figures 5a–b show amorphous $LiNbO_3$ films deposited atop a substrate fully functionalized by the hydrophobic monolayer, except in 4 μm–120 μm wide strips, spaced 250 μm apart. In Fig. 5a, it is apparent the $LiNbO_3$ atop the bare (unfunctionalized) substrate appears dense, while the film above the remainder of the substrate appears crazed and non-uniform in appearance. After nonabrasive polishing with isopropanol, this substrate appears as in Fig. 5b, with the $LiNbO_3$ only adhering to the stripes of bare substrate, and with the crazed film atop the monolayer completely removed from the monolayer-derivatized

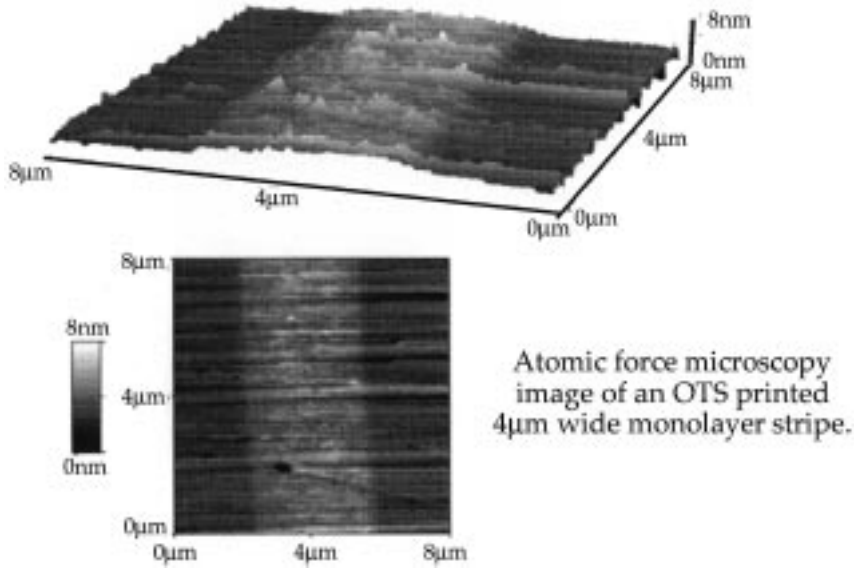

Fig. 4. Topography-mode AFM image of 4 μm wide, 25Å high OTS monolayer on silicon. The monolayer stripe was microcontact printed [2,3].

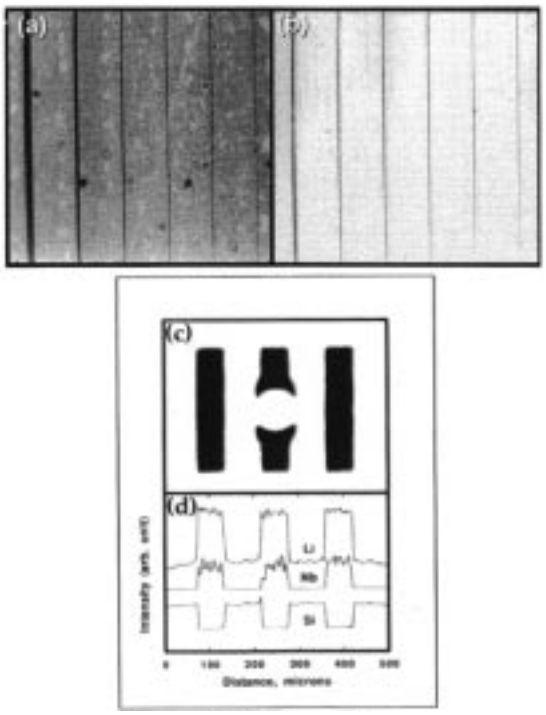

Fig. 5. Optical micrographs (a–c) and Auger electron spectroscopy (d) of selective deposition of $LiNbO_3$ by monolayer patterning.

regions. In Fig. 5c, an optical micrograph of a similarly patterned $LiNbO_3$/Si is shown, along with a line scan for compositional analysis as determined by Auger electron microscopy. It is readily apparent that true selective deposition had been achieved, with a continuous $LiNbO_3$ film on the surface where Si was not functionalized, and with no $LiNbO_3$ present over the functionalized Si.

In pursuit of waveguide applications, films of $LiNbO_3$ were deposited atop OTS-monolayer printed 1 cm [2] sapphire [Al_2O_3 (00.1)] substrates. In this case, the same stripe pattern of Fig. 5b was used to define $\sim$ 100 nm thick, 4–120 nm wide, 1 cm length stripe waveguides. Results of this functionalization, spin coating, 300°C heat treatment, and polishing were similar to those of Fig. 5a–d. Films were then rapidly heated to 700°C to crystalize $LiNbO_3$ heteroepitaxially on sapphire, and these stripe waveguides are shown in Figs. 6a-b. In Fig. 6a, a 1 cm [2] substrate is patterned with 4–120 μm wide-waveguides which are illuminated by uniform side lighting of the structure. In Fig. 6b, a single 100 nm thick, 120 μm wide, >1 cm length $LiNbO_3$ waveguide

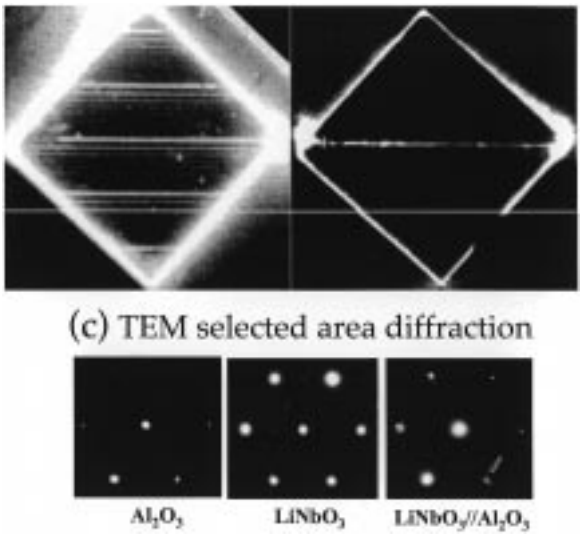

Fig. 6. Heteroepitaxial, monolayer-patterned stripe waveguides of $LiNbO_3$ on sapphire, and selected area electron diffraction.

is shown guiding a TE_0 mode of an end-coupled He-Ne laser. X-ray diffraction, θ rocking curves, and TEM selected area diffraction (Fig. 6c) for this structure confirmed the heteroepitaxial (00.6) $LiNbO_3$//(00.1) Al_2O_3 structure, with mozaic grains aligned to within 0.7° of each other. The combination of integrated, epitaxial, electroceramic films with monolayer patterning [21] enables a new array of potential applications for these materials.

Mechanism of Selective Deposition: Model System Ta_2O_5

Due to the complex evolution of perovskite-type compounds, often including intermediate phase formation such as A-site carbonates or oxy-carbonates, the patterning mechanism was investigated with a single-component metal oxide. Ta_2O_5 is a representative ceramic thin film material, relatively simple in chemical composition, and of interest as a possible higher dielectric constant ($\varepsilon_r = 22$) replacement for SiO_2 ($\varepsilon_r = 3.9$) as gate oxide in integrated circuit devices. The microstructural evolution, stress development, and patterning reliability of Ta_2O_5 thin-film microstructures were investigated to assemble a broader understanding of monolayer-mediated selective deposition of oxide thin films.

Sol-gel precursors for Ta_2O_5 were made from solutions of tantalum ethoxide [$Ta(OCH_2CH_3)_5$,

99.99%, Aldrich] in absolute ethanol, with various solution additions [22]. These solutions were cast by spinning onto patterned or fully OTS monolayer functionalized Si, Pt//Si, Al//Si, TiN, and other substrates using a commercial photoresist spin coater, as described above for $LiNbO_3$. Following low temperature (100–300°C) heat treatment and removal of delaminated oxide, the patterned films were crystallized at 700–800°C, forming crystalline, insulating dielectric thin layers. Films displayed dielectric constants from 18–25 and tan $\delta = 0.007$–0.02 at 1 kHz and 100 mV, with breakdown strengths around 300 kV/cm [22].

The results of prototypical selective deposition of Ta_2O_5 onto an aluminum-coated silicon substrate are shown in Figs. 7 and 8. Solutions of tantalum ethoxide in ethanol, spin coated at 3000 rpm onto an aluminized silicon wafer and heat treated to 300°C, produced selective deposition as shown in the micrographs presented in Fig. 7. The darkest regions are deposited oxide above bare substrate, while the crazed regions are oxide deposited above the hydrophobic monolayer (Fig. 7a). Gentle washing in isopropanol or rubbing with a non-abrasive polishing cloth enabled lift-off of the oxide above the hydrophobic regions, producing the patterned film shown in Fig. 7b. In addition to simple linear shapes, complex patterns of sharp detail were readily formed (Fig. 8a). Fine features as small as 4 μm are readily obtained for 700Å thick layers of Ta_2O_5 (Fig. 8b), with the limiting resolution determined by the efficiency of the lift-off technique. It is noted that the film thickness appears to inversely correlate, in a qualitative manner, with the resolution achieved. Thus it was found that thinner oxide layers enabled higher resolution. This ultimately is expected to enable submicron lateral resolution for the ultrathin dielectric layers that are desired for capacitor, DRAM cell, and interlevel dielectric (ILD) applications. In the current demonstration, a worst case edge resolution of better than $\pm$ 100 nm for 4 μm width shapes was observed, as shown in Fig. 8c. The potential appears to exist for engineering surface topology to optimize edge resolution [22].

Hot-stage ellipsometric studies (Gaertner L116C ellipsometer) for sol-gel Ta_2O_5 thin films deposited on Si indicated that a decrease in thickness occured coincidently with the initial solvent evaporation and that a more gradual densification continued up to 500°C [22]. For a Ta_2O_5 film constrained in the plane

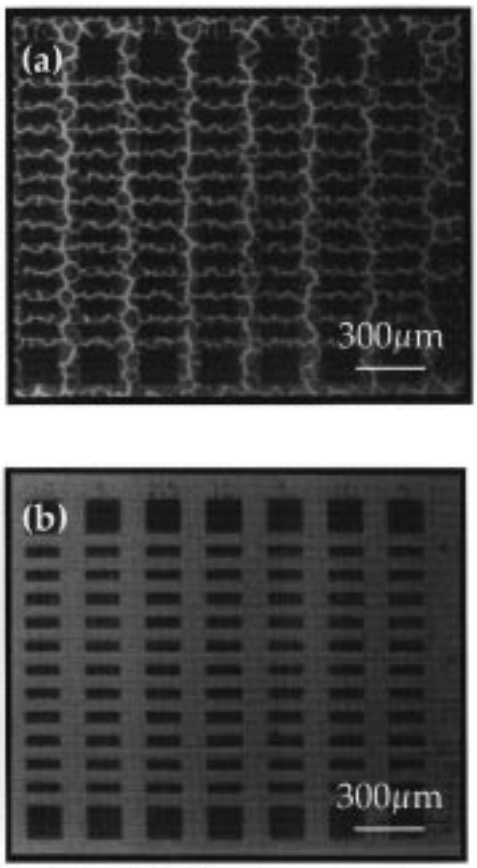

Fig. 7. Tantalum oxide film (a) before and (b) after oxide lift-off [18].

but undergoing volume shrinkage, development of significant tensile stresses would be expected. These stresses appear to play a vital role in the lift off and selective deposition obtained on the functionalized substrates shown in Figs. 7 and 8. Stress analyzes of Ta_2O_5 layers on Si were determined on a hot-stage wafer bending apparatus [23–25] for two limiting cases: (i) Ta_2O_5 deposited directly on Si, and (ii) Ta_2O_5 deposited on a Si wafer bearing a monolayer of OTS across its entire surface. For the case of Ta_2O_5 deposited on unmodified Si, the stress evolution observed on heating followed what might be expected from the ellipsometry data: monotonic increases in stress occur coincidental with shrinkage and densification behavior (Fig. 9a). On cooling to room temperature, these stresses decrease but still remain high—around 100 MPa. This further indicates that the stress evolution was due to constrained volume decrease during densification in addition to the

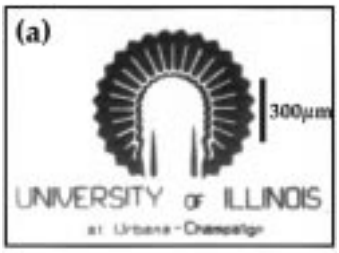

(a) Complex shape patterned Ta_2O_5 thin film on Si

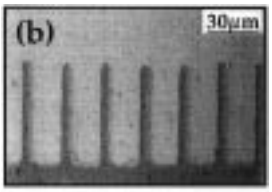

(b) 4μm wide Ta_2O_5 features on Al/Si

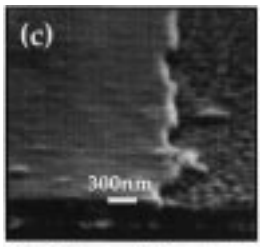

(c) 100nm thick Ta_2O_5 on Al/Si

Fig. 8. Complex shape, fine resolution, and edge structure for monolayer patterned Ta_2O_5 films on Al//Si [18].

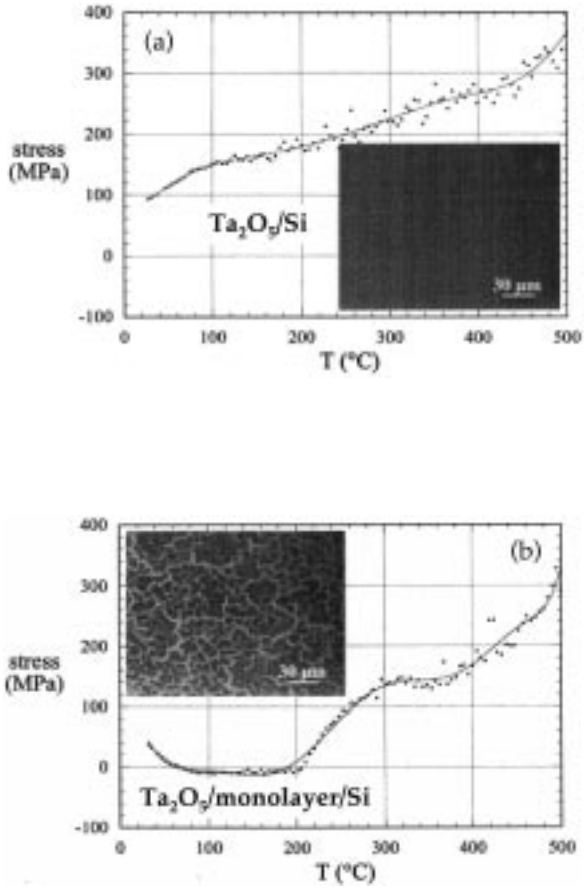

Fig. 9. Stress evolution for $Ta_2O_5//Si$ and Ta_2O_5//monolayer//Si [18].

thermal expansion mismatch between Ta_2O_5 and silicon. This monotonic increase in measured stress contrasts sharply with the stress evolution seen on functionalized surfaces. For these films (Fig. 9b), the thermally-induced apparent stress decreased rapidly, falling to zero during the evaporation step. Above 200°C stresses began to develop, indicating that some modest degree of adhesion is obtained above this temperature despite the presence of the monolayer. The inset micrographs shown in Fig. 9 contrast the dense, high stress Ta_2O_5 films obtained on unfunctionalized Si and the heavily fractured, delaminated, and thus low apparent stress Ta_2O_5 films which form on monolayer-derivatized Si.

The latter data suggest that the mechanism of patterning is closely coupled to that of stress release by film de-adhesion above functionalized regions of the substrate. Similar ellipsometry, stress data, and adhesion behavior were observed for $LiNbO_3$ layers on Si [20] and $PbTiO_3$ on Si. [25] This de-adhesion is readily controllable by the hydrophobic monolayer over a certain temperature window (for Ta_2O_5, around 80–200°C). Below 200°C the delaminated layers remained de-adhered and were readily removed by a variety of methods, such as blowing on or rinsing of the substrate, while above 200°C the increasing mechanical adhesion to the substrate complicated removal, requiring wet, but non-abrasive polishing. This is consistent with earlier work [21], which indicated that in many cases mere washing with isopropanol removed delaminated oxide, while more severe heat treatment required gentle agitation with

cotton felt to remove the weakly bonded, delaminated material. Further experiments to control the state of stress (high stress, low film thickness) for a particular materials system have improved submicron pattern resolution down to a current 0.5 μm feature size.

Monolayer Patterning of Pt//PZT//Pt//Si Ferroelectric Memory Cells

While in many cases, device patterning of oxide material elements is the dominant complication, several other classes of materials also present etching difficulty. While wet chemical etchants exist for noble metals such as silver and gold, platinum patterning typically requires reactive ion etching or imprecise lift-off techniques. As platinum is also the dominant electrode used for fabrication of integrated PZT-based ferroelectric nonvolatile random access memories (NVRAM or FERAM [26]), monolayer patterning may be a natural solution to the difficulty of patterning both Pt and PZT for multilayer Pt//PZT//Pt//Si FERAM device architectures. SAM control of surface character has been used to direct the deposition of MOCVD metals, including Cu [27–28], Pd [29] and Pt [29]. The same mechanism was used to demonstrate device patterning of working multimaterial FERAM cells [18].

For this device, a two layer mask/stamp set was developed, with one monolayer pattern defining the deposition of both the bottom Pt electrode and the PZT cell, and a second monolayer pattern defining the top Pt electrode. The process flow for monolayer patterning and material deposition is shown in Fig. 10. Following microcontact printing of an initial monolayer of OTS on a TiN//Si(100) wafer, an 800Å Pt film was selectively deposited by MOCVD from a bis(hexafluoroacetylacetonato)platinum [$Pt(hfac)_2$] [29] precursor at 350°C and 0.5 torr [18]. As the monolayers are robust up to 400°C, the same monolayer resist was subsequently used to define

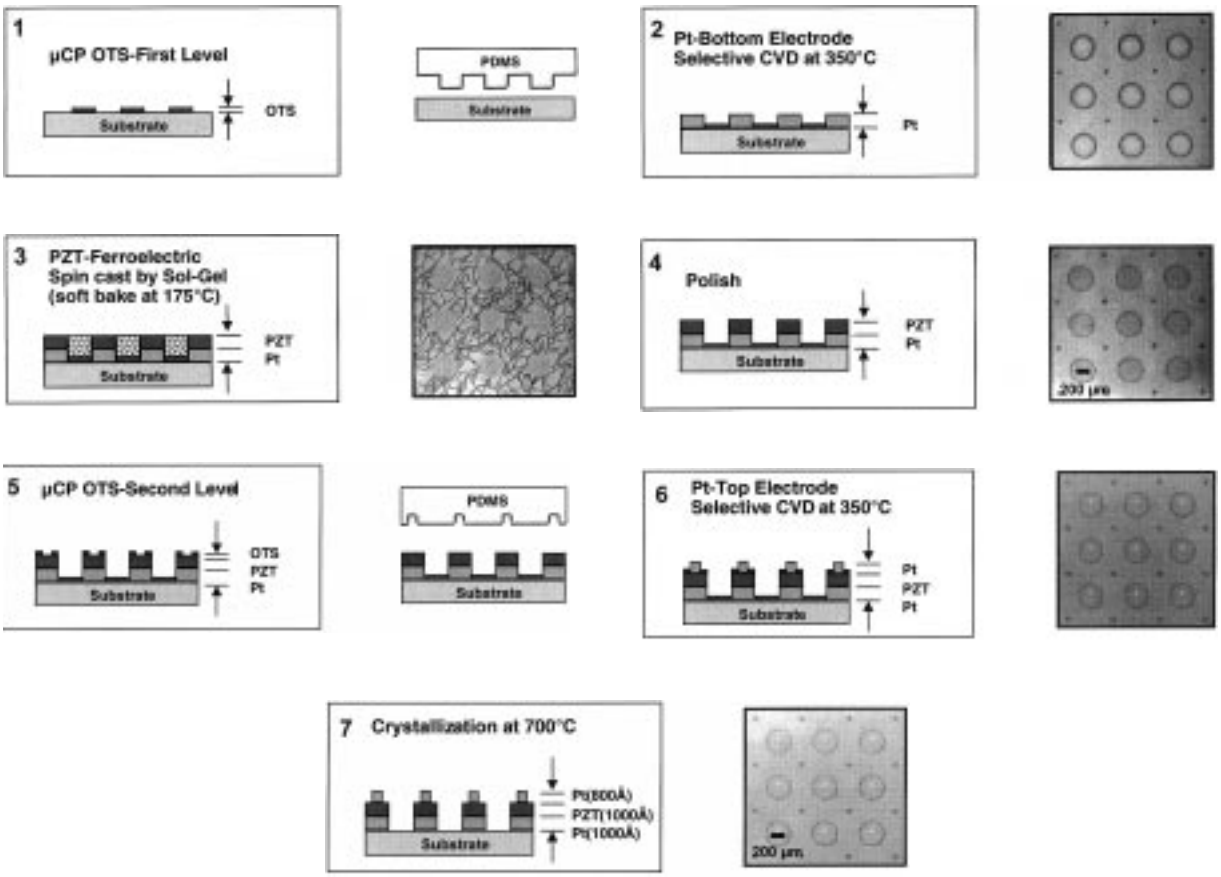

Fig. 10. Schematic of two-stage μCP patterning of Pt//PZT//Pt//TiN//Si ferroelectric memory cells [18].

the deposition of a PZT film, deposited by spin-coating a 0.3 M methoxyethanol-based $PbZr_{0.53}Ti_{0.47}O_3$ sol-gel precursor. Following pyrolysis of the PZT film to 175°C, the PZT deposited above the monolayer functionalized regions subsequently de-adhered and cracked, as observed previously for Ta_2O_5 layers in Fig. 7. These poorly adhered, crazed regions were removed by polishing the entire wafer with cotton felt wet by isopropanol, leaving patterned PZT//Pt structures on the Si substrate. At this point, the second stamp pattern was used to microcontact print OTS monolayers atop the PZT, and selective deposition of Pt was again carried out to define the composite Pt//PZT//Pt//TiN//Si(100) structure. At this point, the entire structure was fired to 700°C to crystallize the PZT and produce a working device structure. A profilometry cross section and the ferroelectric hysteresis characteristics of the multilevel device are shown in Fig. 11. It appears this same methodology could be applied to a broad variety of metal and ceramic systems for device

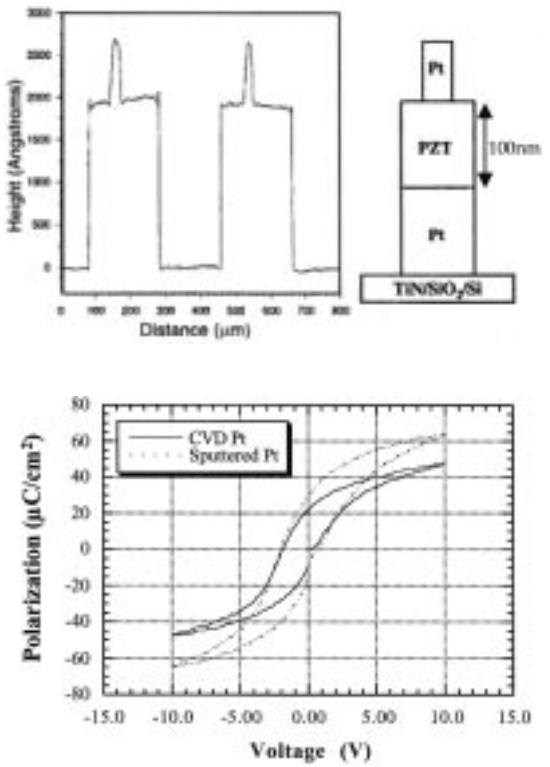

Fig. 11. Profilometry, illustration, and ferroelectric hysteresis for a monolayer patterned FERAM cell [18]. Hysteresis is compared with a standard cell processed with sputtered Pt top and bottom electrodes.

patterning without the need for lithography, wet chemical etching, or reactive ion etching of films. The additive deposition and lift-off process has many practical advantages over conventional subtractive etch processes.

4. Summary

Use of microcontact printing to define patterns of self-assembled monolayers appears to be a promising new method for patterning electroceramics for functional applications, including, integrated capacitors, optical waveguides, ferroelectric memory elements, etc. To date, this method has proven effective in patterning films deposited by several techniques, including sol-gel and MOCVD. It is expected other techniques, including electrodeposition and hydrothermal processing, might also find applications for this method. The robust nature of self-assembled monolayers typically maintain a subtrate's patterned surface character to 400°C, allowing for a variety of deposition processing conditions. Alternatively, the SAMs may be intentionally removed either by heating above this temperature, or by treatment in UV/ozone to decompose the SAM. Perhaps the largest advantage of microcontact printing is the straightforward, ambient processing method amenable to a wide variety of materials. As the patterning is a non-serial, physical stamping method, the potential for high throughput exists and there is no fundamental optical size limit. In particular, patterned features in the 35–40 nm range have been developed by this method [10–11]. The ability to pattern such fine feature sizes bodes well for the integration of electroceramics and other smart materials into many future generations of microelectronics and microelectromechanical systems (MEMS), and is not limited to planar surfaces.

Acknowledgments

The research was supported by the U.S. Department of Energy, Division of Materials Sciences (ER 9645439), and the New Energy Development Organization (NEDO). We are grateful for the use of facilities in the Center for Microanalysis of Materials in the Materials Research Laboratory, and in the Beckman Institute for Advanced Science and Technology. Much of this work was carried out in

collaboration with Dr. Noo Li Jeon, Prof. Ralph G. Nuzzo and Prof. Gregory S. Girolami and we are extremely grateful for this interaction. In addition, we wish to thank Dr. Zhengkui Xu for TEM analysis and Dr. Samit Sengupta for stress data acquisition.

References

1. C.D.E. Lakeman and D.A. Payne, *Mater. Chem. Phys.*, **38**, 305 (1994).
2. R.E. Jones and S.B. Desu, *MRS Bull*, **21**, 55 (1996).
3. *Properties of Lithium Niobate*. EMIS Datareview Series, **5**, edited by S.C. Abrahams (INSPEC, New York, 1989).
4. J. Sagiv, *J. Am. Chem. Soc.*, **102**, 92 (1980).
5. A. Ulman, *An Introduction to Ultrathin Organic Films*, (Academic, Boston, 1991).
6. R.G. Nuzzo and D.L. Allara, *J. Am. Chem. Soc.*, **105**, 4481 (1983).
7. A. Kumar and G.M. Whitesides, *Appl. Phys. Lett.*, **63**, 2002 (1993).
8. K.K. Berggren, A. Bard, J.L. Wilbur, J.D. Gillaspy, A.G. Helg, J.J. McClelland, S.L. Rolston, W.D. Phillips, M. Prentiss, and G.M. Whitesides, *Science*, **269**, 1225 (1995).
9. Y. Xia, E. Kim, M. Mrksich, and G.M. Whitesides, *Chem. Mater.*, **8**, 601 (1996).
10. R.J. Jackman, J.L. Wilbur, and G.M. Whitesides, *Science*, **269**, 664 (1995).
11. Y. Xia and G.M. Whitesides, *Angew. Chem. Int. Ed.*, **37**, 550 (1998).
12. S. Brittain, K. Paul, X.M. Zhao, and G. Whitesides, *Physics World*, **11**, 31 (1998).
13. Y. Xia, D. Qin, and G.M. Whitesides, *Adv. Mat.*, **8**, 1015 (1996).
14. L. Yan, X.M. Zhao, and G.M. Whitesides, *J. Am. Chem. Soc.*, **120**, 6179 (1998).
15. B.C. Bunker, P.C. Rieke, B.J. Tarasevich, A.A. Campbell, G.E. Fryxell, G.L. Graff, L. Song, J. Liu, J.W. Virden, and G.L. McVay, *Science*, **264**, 48 (1994).
16. R.J. Collins, H. Shin, M.R. DeGuire, A.H. Heuer, and C.N. Sukenik, *Appl. Phys. Lett.*, **69**, 860 (1996).
17. C.D.E. Lakeman and D.A. Payne, *J. Am. Ceram. Soc.*, **75**, 3091 (1992).
18. N.L. Jeon, P. Clem, D.Y. Jung, W. Lin, G. Girolami, D.A. Payne, and R.G. Nuzzo, *Adv. Mat.*, **9**, 891 (1997).
19. P.G. Clem and D.A. Payne, in *Ferroelectric Thin Films IV*, edited by S.B. Desu, B.A. Tuttle, R. Ramesh, and T. Shiosaki, *MRS Symp. Proc.* **361**, (Pittsburgh, PA, 1995) p. 179.
20. P.G. Clem, *Ph.D. Thesis*, (University of Illinois, Urbana, IL, 1996).
21. N.L. Jeon, P.G. Clem, R.G. Nuzzo, and D.A. Payne, *J. Mater. Res.*, **10**, 2996 (1995).
22. P.G. Clem, N.L. Jeon, R.G. Nuzzo, and D.A. Payne, *J. Am. Ceram. Soc.*, **80**, 2821 (1997).
23. G.G. Stoney, *Proc. Royal Soc. of London*, **A42**, 172 (1909).
24. S.S. Sengupta, *Ph.D. Thesis*, (University of Illinois, Urbana IL, 1996).
25. S.S. Sengupta, S.M. Park, D.A. Payne, and L.H. Allen, *J. Appl. Phys.*, **83**, 2291 (1998).
26. J.F. Scott and C.A.P. Araujo, *Science*, **246**, 1400 (1989).
27. N.L. Jeon, R.G. Nuzzo, Y. Xia, M. Mrksich, and G.M. Whitesides, *Langmuir*, **11**, 3024 (1995).
28. N.L. Jeon, P.G. Clem, R.G. Nuzzo, and D.A. Payne, *Langmuir*, **12**, 5350 (1996).
29. N.L. Jeon, W.B. Lin, M.K. Erhardt, G.S. Girolami, and R.G. Nuzzo, *Langmuir*, **13**, 3833 (1997).